THE JOURNAL OF
PHYSICAL CHEMISTRY B

ARTICLE

pubs.acs.org/JPCB

Solvation Structure and Dynamics of *cis*- and *trans*-1,2 Dichloroethene Isomers in Supercritical Carbon Dioxide. A Molecular Dynamics Simulation Study.

Dimitris Dellis,*[,†,§] Ioannis Skarmoutsos,*[,‡] and Jannis Samios*[,†]

[†]University of Athens, Department of Chemistry, Laboratory of Physical Chemistry, Panepistimiopolis 157-71, Athens, Greece
[‡]Department of Chemistry, Imperial College London, London SW7 2AZ, United Kingdom

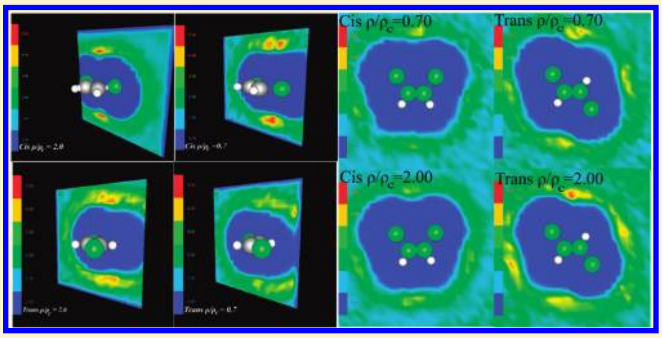

ABSTRACT: Molecular dynamics simulation techniques have been employed to investigate the solvation structure and dynamics in dilute mixtures of *cis*- and *trans*-1,2-dichloroethene in supercritical carbon dioxide. The calculations were performed for state points along a near-critical isotherm (1.02 T_c) over a wide range of densities, using new developed optimized potential models for both isomers. The similarities and differences in the solvation structures around each isomer have been presented and discussed. The local density augmentation and enhancement factors of CO_2 around the isomers have been found significantly larger than the corresponding values for pure supercritical CO_2. The dynamic local density reorganization has been investigated and related to previously proposed relaxation mechanisms. The density dependence of the calculated self-diffusion coefficients has revealed the existence of a plateau in the region of 0.7−1.1 ρ_c, where the local density augmentation exhibits the maximum value. The reorientational dynamics of the C═C bond vector have been also studied, exhibiting significant differences between the two isomers in the case of the second-order Legendre time correlation functions.

I. INTRODUCTION

It is widely known nowadays that the unique properties of supercritical fluids (SCF), for example, adjustable solvation power and dielectric permittivity, low viscosity and surface tension, high diffusivity, etc., are closely related to their characteristic inhomogeneous structure.[1−4] The peculiarity in the behavior of the properties of these molecular systems is that they can be varied continuously and markedly from gaslike to liquidlike values even with a small change in pressure or temperature. Also, the existence of density inhomogeneities in SCF affects significantly their compressibility. As a result of this, large variations in their bulk density can be obtained even with very small pressure changes, causing thus corresponding changes in the solvation of different categories of solutes in supercritical (SC) solvents.

The local solvation structure and especially the local density augmentation[4] (LDA) effects of several, mainly dilute, supercritical solutions have been investigated by employing experimental techniques,[5−13] statistical mechanical theories[14−19] and molecular simulations.[20−30] These studies have revealed important information about the solvation in SCFs.

In two recent vibrational Raman spectroscopic studies,[31,32] Kajiya et al. have tried to analyze the effect of the conformation of solutes on their solvation structure in SCFs. More specifically, they measured the vibrational Raman spectra of the C═C stretching modes of the cis- and trans- isomers of 1,2 dichloroethene (DCE) in SC CO_2 at three isotherms ($T_r = T/T_c$=1.02, 1.06, 1.20) by varying the reduced density of the fluid $\rho_r = \rho/\rho_c$ in the range 0.06−1.57ρ_r and at a fixed solute fraction, where T_c and ρ_c are the critical temperature and density of CO_2, respectively. According to the reported spectra, as the fluid density increases the location of the peak frequencies is shifted toward the low-energy side. Further to this, the authors decomposed these peak frequency shifts in attractive and repulsive components using perturbed hard-sphere theory.[33] Note also that the amounts of the repulsive shifts are found to be almost equivalent for both isomers, whereas those of the attractive shifts of the nonpolar trans-isomer are significantly greater than those of the polar cis-isomer at all densities and temperatures studied. Moreover, by introducing a specific analysis of these attractive shifts, taking also into account the relative orientations between the solute and solvent CO_2 molecules, they pointed out that the anisotropic solvation around the trans- isomers by the CO_2 species could be mainly responsible for the larger attractive shifts in this case.

In recent years, intensive experimental as well as theoretical efforts have been made targeted in predicting detailed information with regard to the intermolecular structure of more complex solutions in condensed phases. To this point, it is generally recognized that among the most powerful tools in predicting in details the intermolecular structure of solutions in condensed phases are the well-known molecular simulation techniques.

Received: May 6, 2011
Revised: August 16, 2011
Published: September 13, 2011

Using these techniques several authors have provided important information about the local density inhomogeneities (LDI) in pure SCF,[4,34−39] as well as in SC solutions.[20−30] Furthermore, in our previous studies we have focused on the static and dynamic behavior of aforementioned LDIs and residence dynamics in pure SCFs,[4,35−39] and the effect of intermolecular interactions upon them.[4]

To the best of our knowledge, computer simulation (CS) studies devoted to the short-range solvation properties and dynamics in the case of solutes existing as isomers in various solvents, specifically at SC conditions, are very scarce in the literature up to now. In connection to this kind of the above-mentioned CS studies of liquid mixtures, it is interesting to mention at this point our previous studies on this field, namely a recent molecular dynamics (MD) treatment of our group devoted to the study of liquid NMF simulated as a mixture of the cis- and trans-NMF isomers.[40] It should be stressed that our main motivation to study this system as a mixture has relied on the results reported in previous experimental studies of this fluid. Concretely, among the results obtained it has been shown that the different local structure around the cis- and trans-NMF isomers is possibly responsible for the observation of different diffusion coefficients at the neat liquid.[40,41] On the other hand, following the literature we may notice that Neutron or X-ray diffraction as well as CS studies of *cis*- and *trans*-1,2-DCE isomers in SC CO_2, directed toward the structural properties of the fluid at different conditions, are not available so far. Therefore, it is very interesting to employ CS techniques to investigate properties of interest of this SC solution aiming to provide useful information related to the effect of the solute isomerism upon them. Thus, in view of this situation we decided here to explore the solvation structure and corresponding dynamics of these two isomers in SC CO_2 by employing the MD simulation technique. In general, the main purpose of the present treatment is to provide further insight into the intermolecular local structure and dynamics of the aforementioned SC solutions in dependence of the fluid bulk density, based on a different methodology from the *vibrational Raman* spectroscopic method used previously,[31,32] namely on the employment of the MD atomistic simulation technique. Note also that particular attention has been paid to the interactions between each isomer solute and the solvent molecules as well as to examine the suggestion made by the authors in refs 31 and 32 with regard to the characteristic solvation structure of each solute (*cis*- and *trans*-1,2-DCE) in the SC solution by the CO_2 solvent. Finally, due to the complete lack of theoretical or experimental data regarding the dynamical properties of the fluid, the corresponding translational and reorientational dynamics of both *cis*- and *trans*-DCE isomers were also investigated. Further to this, the effects of of the solvation structure around the *cis*- and *trans*-DCE species upon their dynamics were also explored.

The rest of the paper is organized as follows: the computational details of the performed simulations are presented in Section II. The results obtained and the following discussion upon them is presented in Section III. Finally, Section IV contains the general conclusions and remarks drawn from the present study.

II. COMPUTATIONAL DETAILS

A. Force Field. It is clear that the performance of computer simulations of molecular systems is strongly dependent, among other fundamental issues, on the selection of the force field employed to model accurately the interactions between the system constituents like atoms, molecules, etc. However, the majority of the existing force fields in the literature have been parametrized to mainly describe liquid state properties and their transferability in different fluid phases has not been widely tested. Therefore the development of methods which ensure the transferability of classical force fields in several fluid phases becomes indispensable.

In the present treatment and because of the binary character of the investigated SC mixtures, one needs to select and employ in the calculations reliable force fields to describe the solvent−solvent, solute−solute and solvent−solute intermolecular interactions. To realize the target of this study, for the solvent−solvent, namely CO_2−CO_2 site−site intermolecular interactions, we decided to employ the elementary physical potential model EPM2 proposed previously[42a] and used successfully in a number of simulation studies of pure CO_2 at several thermodynamic state points.[36,42] This well-known reliable site−site potential model includes Lennard-Jones and electrostatic interactions by means of localized partial charges on the atoms of the CO_2 molecule. The interaction parameters between unlike atoms obtained by the geometric mean for both ε and σ.

$$\begin{aligned} U(r_{ij}) &= 4\varepsilon_{ij}\left[\left(\frac{\sigma_{ij}}{r_{ij}}\right)^{12} - \left(\frac{\sigma_{ij}}{r_{ij}}\right)^{6}\right] + \frac{1}{4\pi\varepsilon_0}\frac{q_i q_j}{r_{ij}} \\ \varepsilon_{ij} &= \sqrt{\varepsilon_i \varepsilon_j} \\ \sigma_{ij} &= \sqrt{\sigma_i \sigma_j} \end{aligned} \qquad (1)$$

Another objective in this part of the present treatment has been the selection of the potential model used to describe the solute−solute interactions, namely among the *cis*- or *trans*-1,2-DCE solutes in the solutions. To the best of our knowledge, there are no systematically constructed specific potential models for these two isomer molecules up to now in the literature, except the case of some generic force fields of OPLS type.[43] However, the OPLS force field description for DCE, overestimates the dipole moment of the cis isomer by a value of 3.09 D compared with the experimental one of 1.90 D.[44] In addition, trial MD simulations on the basis of such OPLS model have revealed that the macroscopical thermodynamic properties obtained differ significantly comparing with experiment. Specifically, we found that it underestimates the pure liquid density of both pure isomers by 1.3−1.6% in the case of cis isomer and by 2.3−2.7% for the trans one. Therefore, at this stage our first task in our MD treatment has been to employ an accurate model for the interactions among the solute molecules in the solutions. Thus, a new rigid force field was developed for both DCE isomers. The main aim of developing a new force field was to reproduce the experimental dipole moment of *cis*-DCE and accurately predict the available thermodynamic experimental data.[44−46] To do so, a combined method including quantum chemical calculations and force field parameters optimization was employed. The *cis*- and *trans*-DCE optimized geometries were obtained by performing quantum chemical ab initio calculations at the MP2 level of theory and employing the cc-pVTZ basis set. The atomic charge distributions were obtained by performing single point energy calculations for the optimized structures and employing the CHELPG[47] method. All the quantum chemical calculations were carried out using the GAMESS[48] package. Further to this, the resulting partial charges, which give a dipole moment for the cis-isomer of 2.24 D, were scaled afterward to reproduce the experimental gas-phase dipole moment of cis-DCE (1.9 D). The geometric characteristics, as well as the final partial charges of cis and trans isomers obtained, are presented in Table 1. Using these partial charges, an optimization procedure[39,49] of the van der Waals parameters ε and σ was applied for pure *cis*- and *trans*-DCE. Since the EPM2[42] force field was used for CO_2, the same functional form and unlike site combination rules were used for the rigid DCE force field. This procedure is based on the minimization over of the dimensionless quantity

$$F(\varepsilon, \sigma) = \frac{1}{N} \sum_{i=1}^{N} \left(\frac{\rho_i^{\text{sim}}(\varepsilon, \sigma) - \rho_i^{\text{exp}}}{\rho_i^{\text{exp}}} \right)^2 \qquad (2)$$

where N is the number of state points, ρ_i^{exp} is the experimental density of the state i, and $\rho_i^{\text{sim}}(\varepsilon,\sigma)$ is the simulated density of the state i using the parameters set (ε,σ) for all different atom types. Experimental data points at normal pressure were taken from references.[44−46] From this procedure, the ε and σ parameters of C, H, and Cl atoms of *cis*- and *trans*-DCE were obtained. These parameters are also presented in Table 1. For the force field evaluation and optimization MD runs carried out in the NPT ensemble, Nose−Hoover[50a,b] thermostat and Parrinello−Rahman barostat[50c] were used with relaxation times 0.2 and 2 ps, respectively. In all simulations, 1000 DCE molecules were used in a cubic box with periodic boundary conditions. The Leapfrog algorithm was employed to solve the equations of motion with time step 1 fs for 1 ns. The potential cutoff was 15 Å in all cases. Long range corrections beyond potential cutoff were applied for both energy and pressure of the simulated system. The Particle Mesh method was used to handle long-range electrostatic interactions correction. The constructed force field was furthermore verified by simulating two thermodynamic state points of each isomer. The experimental and simulated results obtained from these runs are presented in Table 2. From the data in Table 2, it seems clearly that the force field obtained for both isomers reproduces quite accurately the experimental results[44−46] for both pure liquid *cis*- and *trans*-DCE isomers.

Table 1. New Optimized Force Field Parameters for the *cis*- and *trans*-DCE Isomers

		cis	trans
ε_C	[kJ/mol]	0.2860	
ε_H		0.1311	
ε_{Cl}		1.2591	
σ_C	[Å]	3.3810	
σ_H		2.3980	
σ_{Cl}		3.3960	
q_C	[|e|]	−0.0632	−0.0632
q_H		0.1225	0.1492
q_{Cl}		−0.0593	−0.0860
bond C−C	[Å]	1.334	1.332
bond C−H		0.954	0.946
bond C−Cl		1.707	1.716
angle C−C−H	[deg]	120.16	123.16
angle C−C−Cl		124.35	121.24

B. MD Simulations. As mentioned in Introduction, molecular dynamics simulations were performed to investigate the dilute solutions of the cis- and trans-DCE isomers diluted in supercritical CO_2. The simulated systems were consisted of 10 DCE molecules and 990 CO_2 molecules corresponding to a mole fraction of DCE 1%, as in the experimental study of Kajiya and Saitow.[31] The simulations of both systems were carried out at thermodynamic conditions corresponding to the previously experimentally investigated SC state points of the fluid mixtures. Concretely, the simulations of both systems were carried out at a constant temperature 1.02 T_c (T_c is the critical temperature of CO_2, 304.1 K)[4] and several densities in the range $0.2 - 2\rho_c$ (ρ_c is the critical density of the pure CO_2, 0.4676 g/cm^3).[4] At this point, it should be mentioned that the reduced density values of the simulated dilute mixtures have been expressed in terms of the experimental critical density value. The main reason for this is the accurate prediction of the critical point of the CO_2 fluid on the basis of the aforementioned force field used in our treatment, a result that has been already pointed out in previous studies.[42a] Note however that the prediction of the critical point of a fluid in the framework of simulation is very sensitive to the computational technique used (e.g., Gibbs Ensemble or Histogram Reweighting Monte Carlo, MD, etc.)[42] and is strongly affected by the finite size effects close to the critical point.[42b,c]

Each mixture system was equilibrated for 100 ps and subsequently a 2 ns run was performed to calculate the properties of interest. The leapfrog algorithm was employed to integrate the equations of motion using a time step of 1 fs. Also, the Nose−Hoover[50a,b] thermostat was used to constrain the temperature of the simulated systems with a relaxation time of 2 ps. All the MD runs were performed with the GROMACS package.[51] The comparison of experimental pure CO_2 and simulated dilute SC DCE/CO_2 mixtures pressure is presented in Figure 1. From Figure 1, it seems clearly that the simulated pressure of the dilute mixtures is very close to the experimental pressure of pure CO_2, except the prediction at high densities where we observe an increase in the simulated pressure that might be attributed to the somewhat higher molecular volume occupied by DCE molecules in the mixture compared to the corresponding substituted CO_2 species. Obviously this fact specifically at liquid densities leads to an analogue increase of the intermolecular forces among solute and first neighboring solvents with consequences to the system pressure.

Table 2. Experimental and simulated densities for pure liquid cis- and trans-DCE, using the new developed potential model and the OPLS. All simulated densities uncertainty is less than 0.01 g/cm^3. Calculated potential energies of the systems are also presented for both potential models

system	T [K]	ρ_{exp} [g/cm^3]	$\rho_{\text{sim}}^{\text{ThisWork}}$ [g/cm^3]	$\rho_{\text{sim}}^{\text{OPLS}}$ [g/cm^3]	$U_{\text{sim}}^{\text{ThisWork}}$ [KJ/mol]	$U_{\text{sim}}^{\text{OPLS}}$ [KJ/mol]
cis	293.15	1.2880	1.2781	1.2713	−25.4750	−27.7616
	313.15	1.2550	1.2363	1.2343	−24.3228	−26.6477
trans	293.15	1.2568	1.2571	1.2278	−24.5143	−24.5219
	313.15	1.2194	1.2156	1.1863	−23.3898	−23.3825

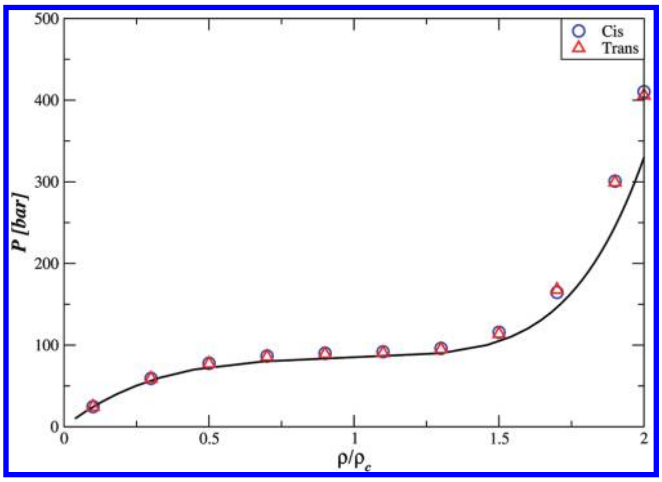

Figure 1. Simulated and experimental pressures of the dilute supercritical mixtures *cis,trans*-DCE-CO_2. Simulated values have been obtained using the new developed potential models (solid line for the experimental results).

III. RESULTS AND DISCUSSION

A. Solvation Structure−Local Density Augmentation. The local structure around the *cis*- and *trans*-DCE isomer solutes in CO_2 has been studied in terms of the calculated center of mass (COM) and atom−atom pair radial distribution functions (PRDFs). In Figure 2, the density dependence of the DCE-CO_2 COM and some representative atom atom PRDF are depicted. The COM DCE-CO_2 PRDF for both the cis and trans isomers are very similar and exhibit the same density dependence. At higher densities the first minimum of these PRDF, that defines the first coordination shell, is more pronounced, clearly indicating the size of the first solvation shell around *cis*- and *trans*-DCE. The first solvation shell at the highest density investigated ($2\rho_c$) is located at 6.6 Å for both isomers. The density dependence of the COM-COM PRDF is very similar to the ones observed for a wide range of pure supercritical fluids.[4,35−37] The shape and density dependence of the DCE-CO_2 atom−atom PRDF is also very similar. In Figure 2b, the most characteristic atom−atom DCE-CO_2 PRDF for both the cis and trans isomers are depicted at a low and a high density (0.3 ρ_c and 2 ρ_c, respectively) indicating the resemblances between the local structures around the cis and trans DCE isomers. In the H-O(CO_2) PRDF a shoulder is located at about 2.9 Å at the highest density investigated, signifying the existence of a weak hydrogen bonding interaction between the DCE isomers and CO_2 solvent at higher densities. This shoulder is slightly higher for the cis isomer. On the other hand, the second peak at about 5.6 Å is slightly higher for trans isomer. At lower densities, this shoulder becomes less pronounced, indicating that these interactions become very weak. In the H-C(CO_2) PRDFs, we observe similar behavior, but in this case the shoulder at about 2.9 Å is a peak rather a shoulder. These observations indicate that the probability to find a solvent atom around H atoms of DCE at distances about 2.9 Å is slightly higher for cis isomer, while at distance about 5.6 Å is higher for trans isomer. This might attributed to the fact that, due to the molecular symmetry and the higher radius of Cl atoms, the two H atoms of cis isomer are more exposed to the solvent than those of the trans isomer. Similar is the behavior of Cl-C(CO_2) and Cl-O(CO_2) PRDFs. In the C(DCE)-O(CO_2) PRDF, we observe a shoulder at 3.7 and 3.8 Å for the cis and trans isomer respectively with no significant differences for both isomers. These observations further support the existence of weak DCE-CO_2 complexes at high densities.

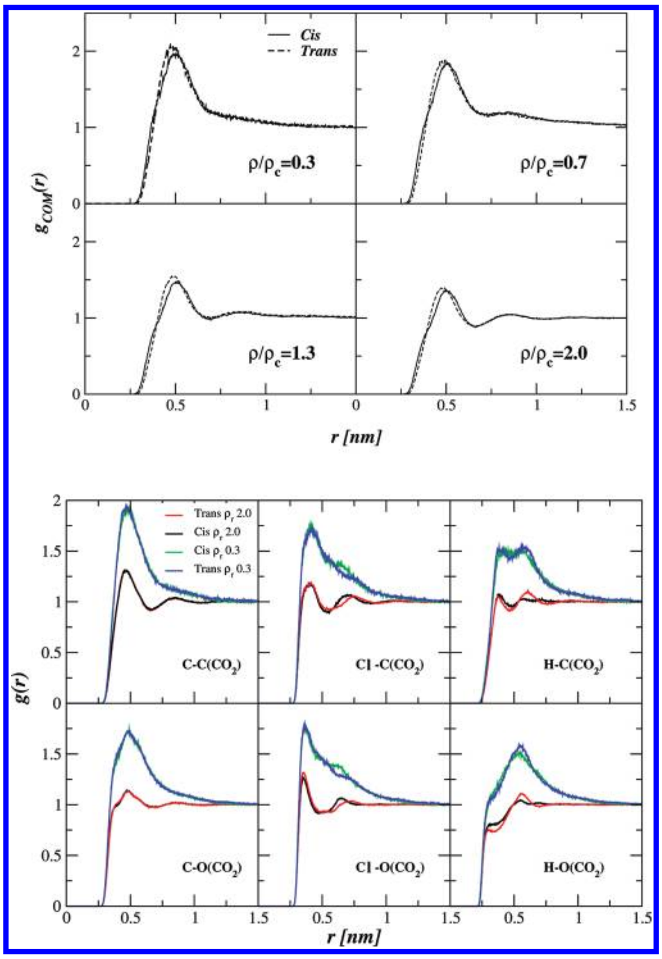

Figure 2. Calculated *cis*-, *trans*-DCE-CO_2 COM-COM and atom−atom PRDF for several representative thermodynamic state points.

To investigate the orientation of the CO_2 molecules around the cis- and trans-DCE isomers, distance and angle distributions characterizing the orientation of CO_2-DCE pairs inside the first solvation shell of each isomer were calculated. Thus the distributions of: the distance between the COM of the C=C bond of each isomer and the carbon of CO_2 (r), the angle between the C=C axis and the vector $r(\theta)$, the angle between the bond axis of CO_2 and the vector $r(\varphi)$, the angle between the C=C axis and the CO_2 axis (ψ), the angle between the vector perpendicular to the plane of DCE and the vector $r(\xi)$, the angle between the vector perpendicular to the plane of DCE and the CO_2 axis (ζ) were obtained for CO_2-DCE pairs inside the first solvation shell of both isomers. The results obtained for the densities of 0.7 ρ_c and 2.0 ρ_c are depicted in Figure 3. From these results it becomes clear that the mean orientation of CO_2 molecules within the first coordination shell of each isomer is very similar. To further investigate the structure of the first coordination shell, the distributions of the distance between the COM of each DCE molecule and the COM of its first coordination shell were calculated for the densities $0.7\rho_c$ and $2.0\rho_c$ and they are presented in Figure 4. These distributions have been found to be very similar for both isomers at the investigated state points. They exhibit a peak at 1.4 Å, indicating that the structural arrangement of CO_2 molecules around

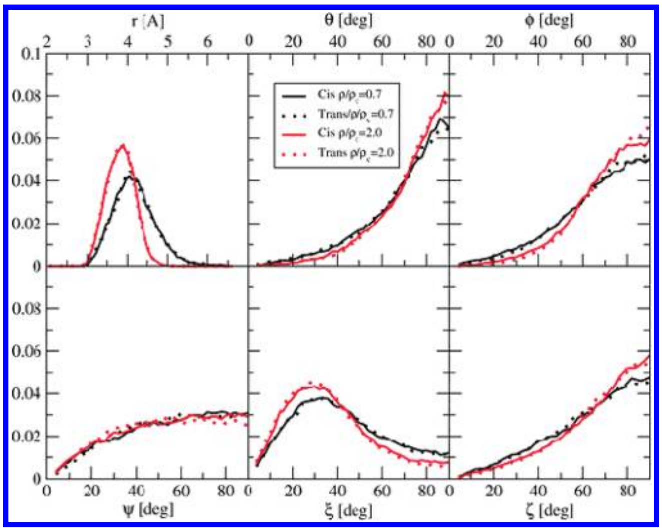

Figure 3. Calculated distance and angle distributions for *cis*-DCE-CO_2 and *trans*-DCE-CO_2 pairs. The symbols used are (a) r = distance between the center of the C═C bond and the COM of CO_2; (b) θ = angle between the C═C axis and the vector r, defined previously; (c) φ = angle between the bond axis of CO_2 and the vector r; (d) ψ = angle between the C═C axis and the CO_2 axis; (e) ξ = angle between the vector perpendicular to the plane of DCE and the vector r; and (f) ζ = angle between the vector perpendicular to the plane of DCE and the CO_2 axis.

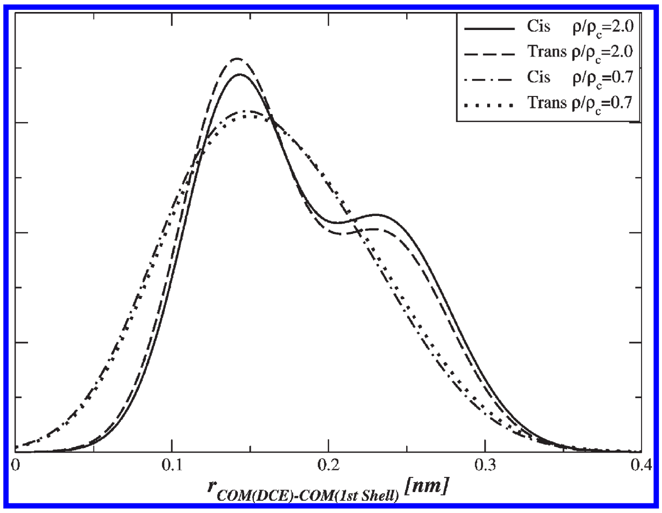

Figure 4. Calculated distributions of the distance between the COM of DCE (cis, trans) and the COM of the first solvation shell of each DCE isomer.

the DCE solutes in their first coordination shell is not spherical. At density 2.0 ρ_c, a shoulder appears close to 2.4 Å. The existence of two peaks in the distributions at high density signifies that as the density increases, the deviation of the shell symmetry from a spherical one becomes larger. Therefore, a second favorable and more asymmetric shell structure appears at high densities, where the distance of the shell's COM from the DCE COM is even larger than in the case of the most favorable structure at low densities. To obtain more detailed information about the local structure around the DCE isomers, the spatial distributions functions (SDF) around them were calculated. In Figure 5a contour plots of SDF, corresponding to a plane perpendicular to the DCE molecule, are presented for both isomers. These plots, although exhibit some small differences between the two isomers, are in general quite similar. In Figure 5b another contour plot of the SDF corresponding to the DCE plane is presented. In this case, differences between the plots corresponding to the two isomers appear at short distances. The distribution of the nearest solvent molecules (green area) around C═C bond is of different symmetry for the cis and trans isomer. The distribution symmetry is the same with the isomers molecular symmetry. These small differences are also reflected in the different shapes of the DCE-CO_2 COM-COM and H-O(CO_2) site−site PRDF corresponding to each isomer at short distances (Figure 2). At longer distances in the first coordination shell the probabilities of finding a solvent molecule around each isomer are very similar (light blue area).

These observations are very significant, since the differences in the attractive shift components of the Raman C═C stretching mode of *cis*- and *trans*-DCE had been attributed to the anisotropic solvation around each isomer in a recent experimental study.[32] The findings of the present study indicate that the orientation of CO_2 molecules around *cis*- and *trans*-DCE inside the first coordination shell is quite similar, but on the other hand, the nearest solvent molecules distribution is quite different for the two isomers.

In the present study, the local density augmentation of CO_2 around *cis*- and *trans*-DCE was also estimated by calculating the average *effective local density*, $\rho_{\mathrm{eff,l}}$, of CO_2 around each isomer. The use of effective local densities to investigate local density inhomogeneities in supercritical fluids has been extensively discussed and justified in previous publications.[5,33,35−37] The calculation of the *effective* local densities was based upon the calculation of the average coordination number N_c corresponding to the first minimum of the DCE-CO_2 COM-COM PRDF

$$N_c(\rho, R_c) = 4\pi\rho \int_0^{R_c} g_{\mathrm{com}}(r) r^2 \, \mathrm{d}r \tag{3}$$

In this equation, $g_{\mathrm{com}}(r)$ is the COM PRDF, and ρ is the bulk number density of the fluid. The cutoff distance R_c is determined as the position of the first minimum of the corresponding g_{com} is observed at a high reference density ρ_{ref} and, in this specific case, has the value of R_c is 6.62 Å for both systems. The employed reference density, ρ_{ref}, corresponds typically to a high liquid-like density and has been set equal to $2\rho_c$. The *effective* local density, $\rho_{\mathrm{eff,l}}$, corresponding to each bulk density has been calculated using the relation

$$\rho_{\mathrm{eff,1}}(\rho, R_c) = \frac{N_c(\rho, R_c)}{N_c(\rho_{\mathrm{ref}}, R_c)} \rho_{\mathrm{ref}} \tag{4}$$

By calculating the *effective local densities*, the excess local density of CO_2 around both isomers was estimated by calculating the *local density augmentation* (LDA), $\Delta\rho_{\mathrm{eff,l}}/\rho_c = (\rho_{\mathrm{eff,l}} - \rho)/\rho_c$, and the *local density enhancement* (LDE), $\rho\mathrm{eff},l/\rho$, factors. The calculated LDA and LDE values for the first solvation shell of both isomers, together with the density dependence of the coordination numbers are depicted in Figure 6. Note that the lines in this figure represent the fitted Weibull (in the case of the LDA) function

$$\Delta\rho_{\mathrm{eff},1}/\rho_c = a\left(\frac{c-1}{c}\right)^{(1-c)/c}\left[\frac{\rho-\rho_0}{b} + \left(\frac{c-1}{c}\right)^{1/c}\right]^c$$
$$\exp\left\{-\left[\frac{\rho-\rho_0}{b} + \left(\frac{c-1}{c}\right)^{1/c}\right]^c + \frac{c-1}{c}\right\} \tag{5}$$

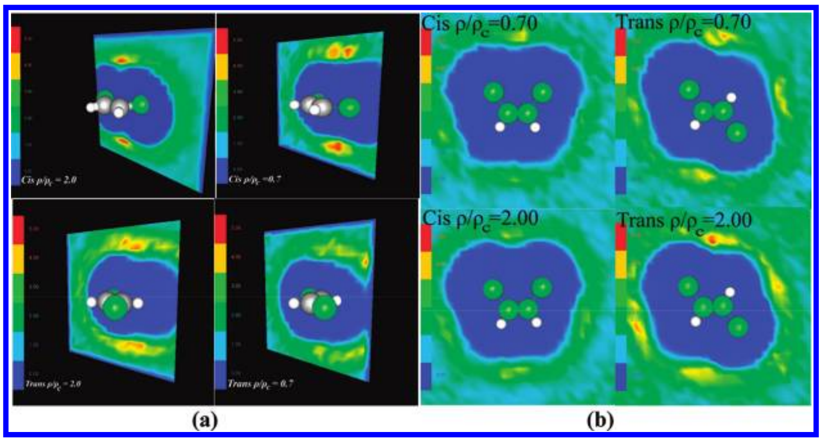

Figure 5. Contour plots of the spatial distribution functions of CO_2 around DCE, corresponding to the DCE plane and the perpendicular one for both cis and trans isomers Results obtained for two densities (ρ/ρ_c = 2.0 and 0.7) are presented.

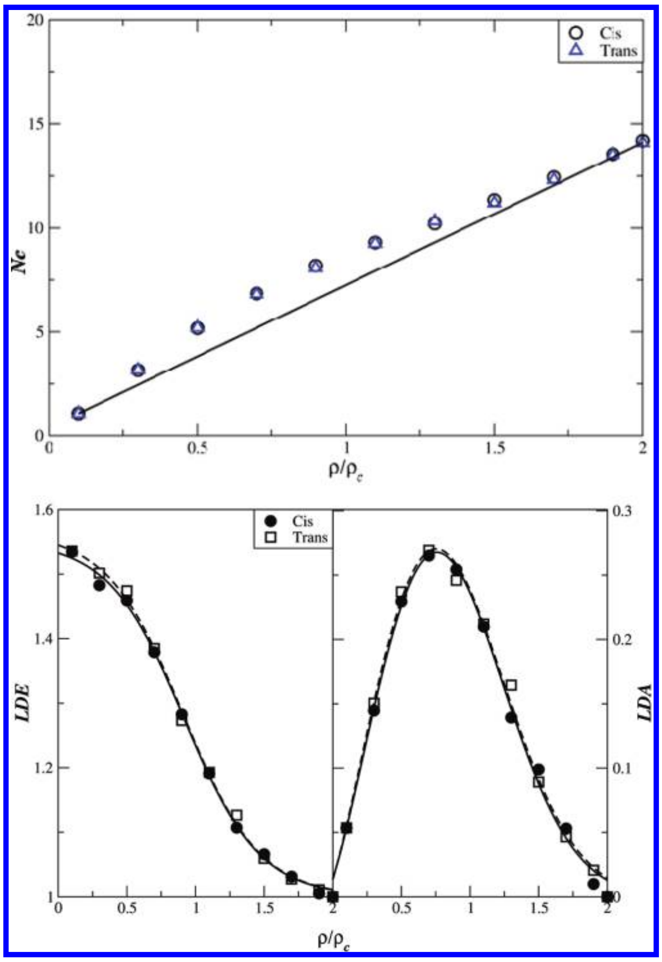

Figure 6. Calculated DCE-CO_2 coordination numbers, LDA and LDE values for the first solvation shell of both isomers.

and the sigmoidal Boltzmann (in the case of LDE)

$$\rho_{\text{eff},1}/\rho = 1 + \left(\frac{a' - 1}{1 + \exp\left(\dfrac{\rho - \rho_0'}{b'}\right)}\right) \tag{6}$$

Table 3. Fitted Parameters of the Weibull and Sigmoidal Boltzmann Functions Used to Model the Local Density Augmentation and Enhancement around of *cis*- and *trans*-DCE, Respectively

Weibull parameters	*cis*-DCE-CO_2	*trans*-DCE-CO_2
α	0.268	0.270
b/ρ_c	1.041	1.037
c	2.311	2.262
ρ_0/ρ_c	0.754	0.754
sigmoidal Boltzmann parameters	***cis*-DCE-CO_2**	***trans*-DCE-CO_2**
a'	1.552	1.566
b'/ρ_c	0.275	0.279
ρ_0'/ρ_c	0.917	0.910

Note that these functional forms, according to our previous findings[4,35−37] have been found very accurate in reproducing the shape of these curves. The parameters of the fitting functions in each case are presented in Table 3. Thus, according to the results obtained the LDA and LDE values of CO_2 around *cis*- and *trans*-DCE are very similar and the LDA values are maximized close to $0.75\rho_c$ exhibiting maximum values of $0.268\rho_c$ and $0.270\rho_c$, respectively. These values are significantly larger for the obtained maximum LDA value of pure CO_2 ($0.09\rho_c$), obtained in previous studies of the authors.[36] This result comes in agreement with previously reported reviews, that in the case of attractive solutes immersed in SC solvents, the average local density of the solvent around the solute is significantly larger than the corresponding value for the pure solvent.[1,5]

B. Local Density Reorganization. Additional insight into the LDA effects in the dilute solutions of cis- and trans-DCE in SC CO_2 may be provided by the investigation of the time dependent distribution of the local density of CO_2 around each isomer. The local density reorganization times, $\tau_{\Delta\rho_l}$, of CO_2 were therefore obtained for both solutions, by integrating the calculated local density time correlation functions (TCF) $C_{\Delta\rho_l}(t)$, where $\Delta\rho_l(t)$ is the local-density deviation, relative to the mean local one, and is defined as $\Delta\rho_l(t) = \rho_l(t) - \langle\rho_l\rangle$

$$C_{\Delta\rho,1}(t) = \frac{\langle\Delta\rho_l(0)\cdot\Delta\rho_l(t)\rangle}{\langle|\Delta\rho_l(0)|^2\rangle} \tag{7}$$

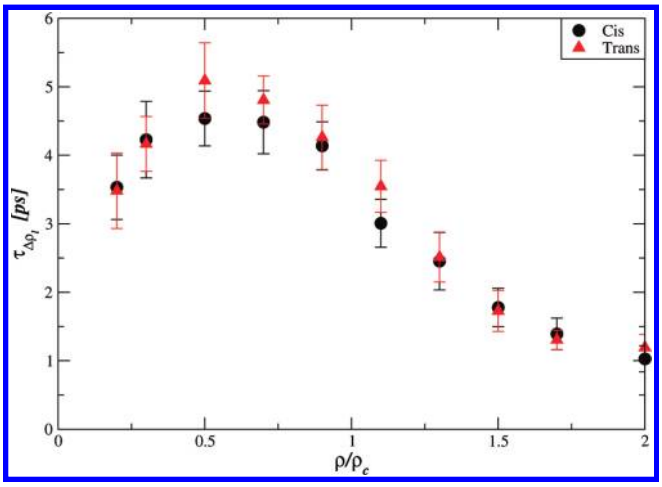

Figure 7. Bulk density dependence of the obtained local density reorganization times $\tau_{\Delta\rho_l}$ of CO_2 in the first solvation shell *cis*- and *trans*-DCE.

In the present treatment, the instantaneous local density $\rho_l(t)$ was calculated using eq 4 at each time t. The correlation time, $\tau_{\Delta\rho_l}$, was determined by the following relation:

$$\tau_{\Delta\rho_l} = \int_0^\infty C_{\Delta\rho_l}(t)\, dt \tag{8}$$

In Figure 7, the bulk density dependence of the obtained local density reorganization times $\tau_{\Delta\rho_l}$ of CO_2 in the first solvation shell of *cis*- and *trans*-DCE are presented. In general, the calculated values of $\tau_{\Delta\rho_l}$ are very similar for both isomers and only in the density range where the LDA is maximized these values are slightly larger in the case of *trans*-DCE. Moreover in Figure 8, a representative 3-dimensional plot depicting the dependence of the calculated $\tau_{\Delta\rho_l}$ values on the cutoff distance of the local region and on the bulk density of the system is presented for both systems. According to the results obtained, the $\tau_{\Delta\rho_l}$ values depend not only on the density of the fluid, but also on the length scale of the region taken into account in the calculations. By extending the cutoff distance around each solute molecule, the reorganization time exhibits maximum values in the density range where the LDA values are maximized. However, this behavior is not apparent at shorter intermolecular distances. At short distances, the number of solvent molecules that are inside the cutoff of the local region decreases. Depending on density, there are 3−15 solvent molecules around DCE molecules at distance less than 6.6 Å, that defines the first coordination shell. At distance less than 5 Å there are 1−5 solvent molecules, while at distance less than 4 Å, there are on average 0.2−1.2 solvent molecules. All these results support previous findings that at more extended length scales, the long-range density fluctuations and related collective effects affect differently the local density reorganization mechanisms than at shorter intermolecular distances, where probably direct intermolecular interactions seem to have a more important contribution.[35−37,39,52] The same behavior has been observed also for pure benzene and hexafluorobenzene.[39] Similar conclusions have been reported also for other systems in our previous publications,[35−37] indicating that this behavior is a universal one.

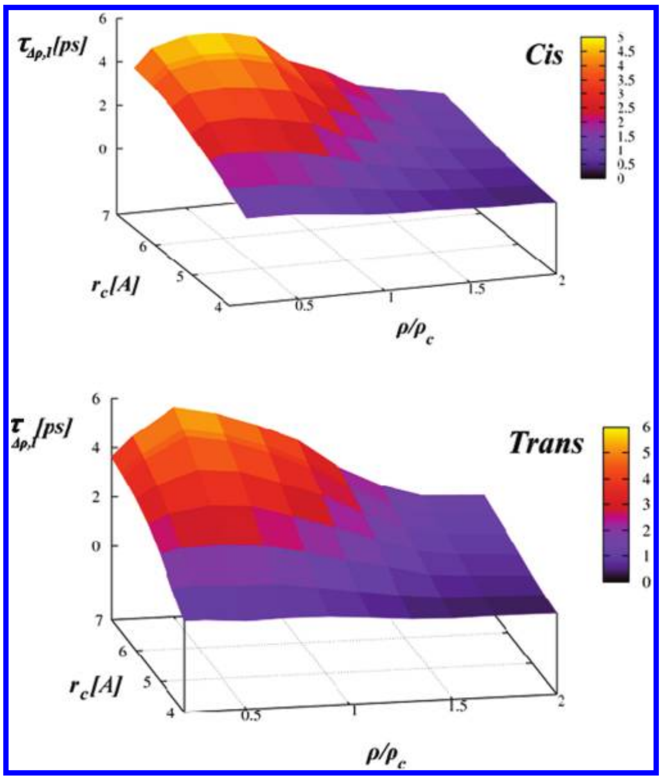

Figure 8. Dependence of the calculated $\tau_{\Delta\rho_l}$ values on the cutoff distance of the local region and the bulk density of the system.

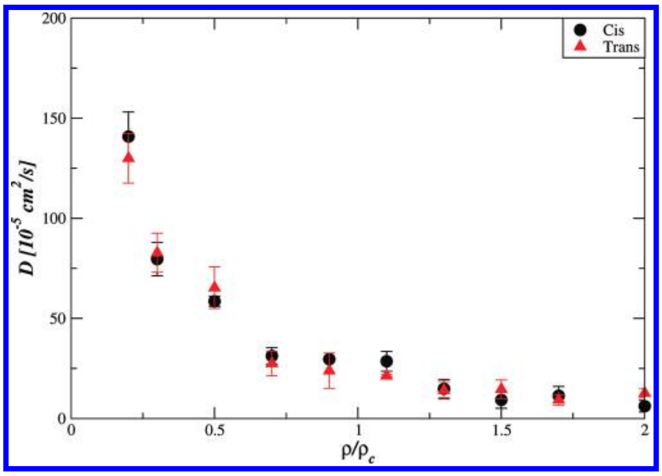

Figure 9. Bulk density dependence of the calculated diffusion coefficients of *cis*- and *trans*-DCE.

C. Translational−Reorientational Dynamics. The translational and reorientational dynamics of the *cis*- and *trans*-DCE molecules has also been examined. The average mean square displacement of both isomer molecules has been computed and used in the Einstein relation to determine the average translational diffusion coefficient

$$D = \frac{1}{6}\lim_{t\to\infty}\frac{1}{t}\langle|\vec{r}_i(0) - \vec{r}_i(t)|^2\rangle \tag{9}$$

The bulk density dependence of the calculated diffusion coefficients of cis- and trans-DCE is presented in Figure 9, exhibiting a very similar behavior. A plateau for the diffusion coefficients in the density region where the LDA and the local density reorganization time are maximized may be observed in this Figure.

A similar behavior has been reported for several dynamic properties of solutes in supercritical solvents.[1,38,53]

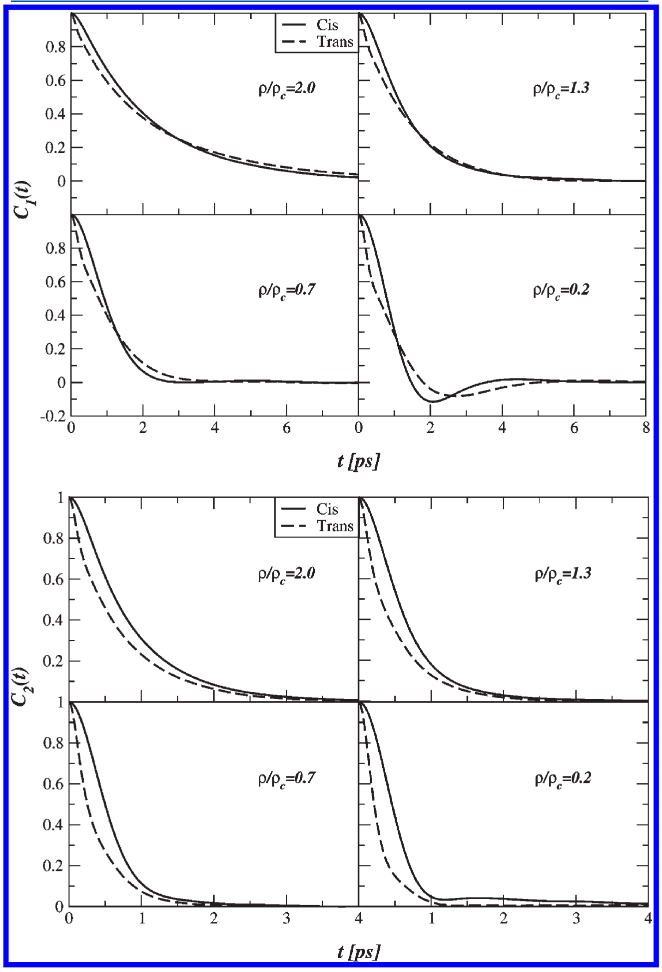

Figure 10. Calculated first and second order Legendre reorientational TCFs for the C=C vectors of *cis*- and *trans*-DCE for some representative state points.

The reorientational dynamics for the C=C intramolecular vectors of *cis*- and *trans*-DCE have been also investigated by means of the Legendre reorientational TCFs

$$C_\ell(t) = \langle P_\ell(\vec{u}(0)\cdot\vec{u}(t))\rangle, \ell = 1, 2 \tag{10}$$

In this equation $\vec{u}$ is a unit vector along the C=C vectors of cis- and trans-DCE and P_ℓ is a Legendre polynomial ($P_1(x) = x, P_2(x) = 1/2(3x^2 - 1)$). The corresponding reorientational times τ_ℓ ($\ell = 1, 2$) are defined as follows:

$$\tau_\ell = \int_0^\infty C_\ell(t)\cdot \mathrm{d}t \tag{11}$$

The calculated first and second order Legendre reorientational TCFs for the C=C vectors of *cis*- and *trans*-DCE and for some representative state points are depicted in Figure 10. It may be clearly observed that at low densities the first order Legendre TCFs $C_1(t)$ exhibit negative parts and this behavior is similar to the free rotor one. This negative part starts to disappear when increasing the density of the solvent and it is not present at higher liquid-like densities, signifying the strong density effects on these dynamics. The calculated reorientational $C_1(t)$ and $C_2(t)$ TCFs for *cis*- and *trans*-DCE exhibit also differences, indicating that the reorientational dynamics of the *cis*- and *trans*-DCE isomers are not the same. In Figure 11 the density dependence of the calculated reorientational correlation times, τ_1 and τ_2, is presented. While the density dependence and the obtained τ_1 values for cis- and trans-DCE are similar, on the other hand the obtained τ_2 values and their density dependence are very different. This is not surprising since the two isomers have different molecular symmetry that implies different moment of inertia tensor. Since the both isomers have similar solvation environment, the forces that act on the DCE molecules from the surrounding solvent molecules is expected to be similar. The difference in the reorientation TCFs and consequently in correlation times, might be attributed to the different moment of inertia of DCE isomers. Such an observation is very interesting, since previous studies have revealed that first order reorientational dynamics are more sensitive to the local environment around a molecule.[36,38]

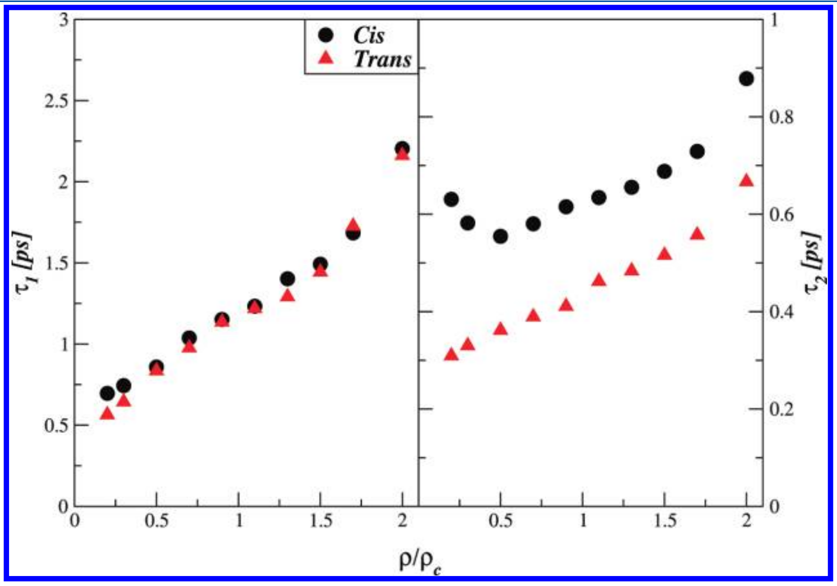

Figure 11. Density dependence of the calculated first and second order reorientational correlation times, τ_1 and τ_2, for the C=C vectors of *cis*- and *trans*-DCE.

Taking into account that the local environments around both isomers have been found to be very similar, the similarities in the behavior of τ_1 is in agreement with the findings of those works. However the different behavior of the calculated τ_2 values and the $C_2(t)$ Legendre reorientational TCFs, indicates that this behavior could affect the shape and position of the Raman and Rayleigh C═C stretching peaks. It is well-known that the Raman and Rayleigh spectral TCFs are related to the changes in the polarizability tensor anisotropy and molecular reorientation, which is expressed in terms of the second order Legendre reorientational TCFs $C_2(t)$. More specifically, they are determined by the correlations of permanent polarizability, interaction induced contributions to the polarizability, orientational correlations of the molecular polarizability anisotropies and cancellation effects resulting by the many-body terms in the cross and collision-induced components of the spectral TCFs.[54−61] Therefore these mechanisms together with the fact that the distribution of the nearest solvent molecules around the C═C bond is of different symmetry, could result different Raman spectral shifts in these dilute supercritical solutions. However, a more detailed study of these mechanisms and how they affect the Raman and Rayleigh spectral shifts is necessary to have a clearer picture about these complicated interaction-induced effects and it is one of our future goals.

IV. GENERAL CONCLUSIONS

In the present treatment, molecular dynamics simulations have been carried out to predict the solvation structure and related properties in dilute solutions of *cis*- and *trans*-DCE in supercritical CO_2. New potential models have been developed for both isomers, employing ab initio quantum chemical calculations and optimization techniques. The local intermolecular structure around both isomers was studied in terms of the atom—atom PRDFs, angle and distance distributions, as well as spatial distribution functions. The results obtained reveal similar structural arrangements of the CO_2 solvent molecules in the first solvation shell of each isomer. However, the calculated SDFs have revealed that the distribution of the nearest solvent molecules around the C═C bond is of different symmetry for cis and trans isomers. At longer distances in the first coordination shell the probability to find a solvent molecule around the *cis*- and *trans*-DCE molecules is very similar.

The local density augmentation and enhancement factors of the CO_2 solvent around each solute were also calculated and their values are much larger in comparison with the corresponding pure CO_2 ones. However, the differences between the two solutes were found to be very small. The time dependent local density reorganization around both solutes has been also investigated and it is found that the calculated local density reorganization times $\tau_{\Delta\rho_l}$ depend not only on the density of the fluid but also on the length scale of the region taken into account in the calculations. By increasing the cutoff distance around each solute molecule, the reorganization time exhibits maximum values in the density range where the local density augmentation values are maximized.

The self-diffusion coefficients of each isomer were also calculated revealing the existence of a plateau in the density region, where the LDA and the local density reorganization time are maximized. A similar behavior has been observed for several dynamic properties of solutes in supercritical solvents.[1,38,53] Finally, the reorientational dynamics for the C═C intramolecular vectors of *cis*- and *trans*-DCE have been also investigated by means of the first- and second-order Legendre reorientational TCFs and the corresponding correlation times. According to the results obtained, the density dependence of the τ_1 values for *cis*- and *trans*-DCE exhibit small differences to each other and with density, but the calculated τ_2 values and their density dependence are significantly different. The calculated reorientational $C_1(t)$ and $C_2(t)$ TCFs for *cis*- and *trans*-DCE exhibit also differences, indicating that the reorientational dynamics of the *cis*- and *trans*-DCE isomers in supercritical CO_2 are different.

■ AUTHOR INFORMATION

Corresponding Author

*E-mail: ntell@chem.uoa.gr (D.D.); i.skarmoutsos@imperial.ac.uk (I.S.); isamios@chem.uoa.gr (J.S.).

Present Addresses

§Institute of Accelerating Systems and Applications, Panepistimiopolis Zografou, 15784, Athens, Greece.

■ REFERENCES

(1) Tucker, S. C. *Chem. Rev.* **1999**, *99*, 391.

(2) Besnard, M.; Tassaing, T.; Danten, Y.; Andanson, J. M.; Soetens, J. C.; Cansell, F.; Loppinet-Serani, A.; Reveron, H.; Aymonier, C. *J. Mol. Liq.* **2006**, *125*, 88.

(3) Kajimoto, O. *Chem. Rev.* **1999**, *99*, 355.

(4) Skarmoutsos, I.; Dellis, D.; Samios, J. *J. Phys. Chem B.* **2009**, *113*, 2783.

(5) Song, W.; Biswas, R.; Maroncelli, M. *J. Phys. Chem. A* **2000**, *104*, 6924.

(6) Lewis, J.; Biswas, R.; Robinson, A.; Maroncelli, M. *J. Phys. Chem. B* **2001**, *105*, 3306.

(7) Lalanne, P.; Tassaing, T.; Danten, Y.; Cansell, F.; Tucker, S. C.; Besnard, M. *J. Phys. Chem. A* **2004**, *108*, 2617.

(8) Aizawa, T.; Kanakubo, M.; Ikushima, Y.; Smith, R. L., Jr; Saitoh, T.; Sugimoto, N. *Chem. Phys. Lett.* **2004**, *393*, 31.

(9) Okamoto, M.; Nagashima, H.; Tanaka, F. *Phys. Chem. Chem. Phys.* **2002**, *4*, 5627.

(10) Rice, J. K.; Niemeyer, E. D.; Dunbar, R. A.; Bright, F. V. *J. Am. Chem. Soc.* **1995**, *117*, 5832.

(11) Knutson, B. L.; Tomasko, D. L.; Eckert, C. A.; Debenedetti, P. G.; Chialvo, A. A. Local Density Augmentation in Supercritical Solutions: A Comparison Between Fluorescence Spectroscopy and Molecular Dynamics Results. In *Recent Advances in Supercritical Fluid Technology: Applications and Fundamental Studies*; Bright, F. V., McNally, M. E. P., Eds; ACS Symposium Series; American Chemical Society: Washington, DC, 1992; Vol. 488; p 60−72.

(12) Betts, T. A.; Zagrobelny, J.; Bright, F. V. *J. Am. Chem. Soc.* **1992**, *114*, 8163.

(13) Heitz, M. P.; Bright, F. V. *J. Phys. Chem.* **1996**, *100*, 6889.

(14) Husowitz, B.; Talanquer, V. *J. Chem. Phys.* **2007**, *126*, 054508.

(15) Perera, A. *J. Chem. Phys.* **2001**, *115*, 6115.

(16) Zhou, S. Q. *J. Phys. Chem. B* **2005**, *109*, 7522.

(17) Egorov, S. *J. Chem. Phys.* **2000**, *112*, 7138.

(18) Egorov, S. A.; Yethiraj, A.; Skinner, J. L. *Chem. Phys. Lett.* **2000**, *317*, 558.

(19) (a) Petsche, I. B.; Debenedetti, P. G. *J. Phys. Chem.* **1991**, *95*, 386. (b) Petsche, I. B.; Debenedetti, P. G. *J. Chem. Phys.* **1989**, *91*, 7075.

(20) (a) Chalaris, M.; Samios, J. *J. Phys. Chem. B* **1999**, *103*, 1161. (b) Chatzis, G.; Samios, J. *Chem. Phys. Lett.* **2003**, *374*, 187.

(21) Debenedetti, P. G.; Petsche, I. B.; Mohamed, R. S. *Fluid Phase Equilib.* **1989**, *52*, 347.

(22) Inomata, H.; Saito, S.; Debenedetti, P. G. *Fluid Phase Equilib.* **1996**, *116*, 282.

(23) Siavosh-Haghighi, A.; Adams, J. E. *J. Phys. Chem. A* **2001**, *105*, 2680.

(24) Nugent, S.; Ladanyi, B. M. *J. Chem. Phys.* **2004**, *120*, 874.

(25) Favero, F. W.; Skaf, M. S. *J. Supercrit. Fluids* **2005**, *34*, 237.

(26) Ingrosso, F.; Ladanyi, B. M.; Menucci, B.; Scalmani, G. *J. Phys. Chem. B* **2006**, *110*, 4953.

(27) Yamaguchi, T.; Kimura, Y.; Hirota, M. *J. Chem. Phys.* **1999**, *111*, 4169.

(28) Yamaguchi, T.; Kimura, Y.; Nakahara, M. *J. Phys. Chem. B* **2002**, *106*, 9126.

(29) Guardia, E.; Laria, D.; Marti, J. *J. Phys. Chem. B* **2006**, *110*, 6332.

(30) Frankland, S. J. V.; Maroncelli, M. *J. Chem. Phys.* **1999**, *110*, 1687.

(31) Kajiya, D.; Mouri, Y.; Saitow, K. *J. Phys. Chem. B* **2008**, *112*, 7980.

(32) Kajiya, D.; Saitow, K. *J. Phys. Chem. B* **2009**, *113*, 13291.

(33) (a) Schweizer, K. S.; Chandler, D. *J. Chem. Phys.* **1982**, *76*, 2296. (b) Zakin, M. R.; Herschbach, D. R. *J. Chem. Phys.* **1986**, *85*, 2376.

(34) (a) Adams, J. E.; Siavosh-Haghighi, A. *J. Phys. Chem. A* **2002**, *106*, 7973. (b) Song, W.; Maroncelli, M. *Chem. Phys. Lett.* **2003**, *378*, 410.

(35) Skarmoutsos, I.; Samios, J. *J. Phys. Chem. B* **2006**, *110*, 21931.

(36) Skarmoutsos, I.; Samios, J. *J. Chem. Phys.* **2007**, *126*, 044503.

(37) Skarmoutsos, I.; Guardia, E. *J. Phys. Chem. B* **2009**, *113*, 8887.

(38) Skarmoutsos, I.; Guardia, E. *J. Phys. Chem. B* **2009**, *113*, 8898.

(39) Dellis, D.; Skarmoutsos, I.; Samios, J. *J. Mol. Liq.* **2010**, *153*, 25.

(40) Skarmoutsos, I.; Samios, J. *Chem. Phys. Lett.* **2004**, *384*, 108.

(41) Chen, L.; Gross, T.; Lüdemann, H. D.; Krienke, H.; Fischer, R. *Naturwissenschaften* **2000**, *87*, 225.

(42) (a) Harris, J. G.; Young, K. H. *J. Phys. Chem.* **1995**, *99*, 12021. (b) Nieto-Draghi, C.; de Bruin, T.; Perez-Pellitero, J.; Bonet Avalos, J.; Mackie, A. D. *J. Chem. Phys.* **2007**, *126*, 064509. (c) Boulougouris, G. C.; Peristeras, L. D.; Economou, I. G.; Theodorou, D. N. *J. Supercrit. Fluids* **2010**, *55*, 503.

(43) Jorgensen, W. L.; Severance, D. L. *J. Am. Chem. Soc.* **1990**, *112*, 4768.

(44) (a) Hahn, G; P. Svejda, P. *J. Chem. Eng. Data* **1996**, *41*, 619.*CRC Handbook of Chemistry and Physics*; Lide, D. R., Eds. CRC Press: Boca Raton, FL., 1994.

(45) Hahn, G; Ulcay, K.; Svejda, P. *J. Chem. Eng. Data* **1996**, *41*, 319.

(46) Comelli, F.; Francesconi, R. *J. Chem. Eng. Data* **1995**, *40*, 1184.

(47) Breneman, C. N.; Wiberg, K. B. *J. Comput. Chem.* **1990**, *11*, 361.

(48) Schmidt, M. W.; Baldridge, K. K.; Boatz, J. A.; Elbert, S. T.; Gordon, M.S. J.H.; Jensen, J. H.; Koseki, S.; Matsunaga, N.; Su, K. S. J.; Windus, T. L.; Dupuis, M.; J.A. Montgomery, J. A. *J. Comput. Chem.* **1993**, *14*, 1347.

(49) Dellis, D.; Samios, J. *Fluid Phase Equilib.* **2010**, *291*, 81.

(50) (a) Nosé, S. *Mol. Phys.* **1984**, *52*, 255. (b) Hoover, W. G. *Phys. Rev. A* **1985**, *31*, 1695. (c) Parrinello, M.; Rahman, A. *J. Appl. Phys.* **1981**, *52*, 7182.

(51) Hess, B.; Kutzner, C.; van der Spoel, D.; Lindahl, E. *J. Chem. Theory Comput.* **2008**, *4*, 435.

(52) Maddox, M. W.; Goodyear, G.; Tucker, S. C. *J. Phys. Chem. B* **2000**, *104*, 6266.

(53) Goodyear, G.; Tucker, S. C. *J. Chem. Phys.* **1999**, *110*, 3643.

(54) Frenkel, D.; McTague, J. *J. Chem. Phys.* **1980**, *72*, 2801.

(55) Ladanyi, B. M.; Keyes, T. *Mol. Phys.* **1977**, *33*, 1063.

(56) Cox, T. I.; Battaglia, M. R.; Madden, P. A. *Mol. Phys.* **1979**, *38*, 1539.

(57) Mueller, A.; Steele, W. A.; Versmold, H. *J. Chem. Phys.* **1993**, *99*, 4993.

(58) *Phenomena Induced by Intermolecular Interactions*; Birnbaum, G., Ed.; Plenum Press; New York, 1985; NATO ASI Ser. B

(59) Gray, C. G.; Gubbins, K. E. *Theory of Molecular Fluids*; Clarendon Press, Oxford, U.K., 1984.

(60) Strehle, F.; Dorfmüller, T.; Samios, J. *Mol. Phys.* **1991**, *72*, 993.

(61) Samios, J.; Mittag, U. *J. Phys. Chem.* **1994**, *98*, 2033.